

Variation of Distributed Power Control Algorithm in Co-Tier Femtocell Network

Fatur Rahman Harahap, Anggun Fitriani Isnawati, Khoirun Ni'amah
Institut Teknologi Telkom Purwokerto, Indonesia

Article Info

Article history:

Received April 22, 2024
Revised July 17, 2024
Accepted September 15, 2024

Keywords:

*Co-Tier Femtocell Network
Convergence
Distributed Power Control
Feasibility
Power Treatment*

ABSTRACT

The wireless communication network has seen rapid growth, especially with the widespread use of smartphones, but resources are increasingly limited, especially indoors. Femtocell, a spectrum-efficient small cellular network solution, faces challenges in distributed power control (DPC) when deployed with distributed users, impacting power levels and causing interference in the main network. This research aims to optimize user power consumption in co-tier femtocell networks using the user power treatment. This study proposed the Distributed Power Control (DPC) variation methods such as Distributed Constrained Power Control (DCPC), Half Distributed Constrained Power Control (HDCPC), and Generalized Distributed Constrained Power Control (GDCPC) in co-tier femtocell network. The research examines scenarios where user power converges but exceeds the maximum threshold or remains semi-feasible, considering factors like number of users, distance, channel usage, maximum power values, non-negative power vectors, Signal-to-Interference-plus-Noise Ratio (SINR), and link gain matrix values. In Distributed Power Control (DPC), distance and channel utilization affect feasibility conditions: feasible, semi-feasible, and non-feasible. The result shows that Half Distributed Constrained Power Control (HDCPC) is more effective than Distributed Constrained Power Control (DCPC) in semi-feasible conditions due to its efficient power usage and similar Signal-to-Interference-plus-Noise Ratio (SINR). Half Distributed Constrained Power Control (HDCPC) is also easier to implement than Generalized Distributed Constrained Power Control (GDCPC) as it does not require user deactivation when exceeding the maximum power limit. Distributed Power Control (DPC) variations can shift the power and Signal-to-Interference-plus-Noise Ratio (SINR) conditions from non-convergence to convergence at or below the maximum power level. We concluded that the best performance of Distributed Power Control (DPC) is Half Distributed Constrained Power Control (HDCPC).

Copyright ©2024 The Authors.
This is an open access article under the [CC BY-SA](#) license.



Corresponding Author:

Anggun Fitriani Isnawati,
Telecommunications and Electrical Engineering,
Institut Teknologi Telkom Purwokerto, Indonesia,
Email: anggun@ittelkom-pwt.ac.id

How to Cite:

F. R. Harahap, A. F. Isnawati, and K. Ni'amah, "Variation of Distributed Power Control Algorithm in Co-Tier Femtocell Network", *MATRIK: Jurnal Manajemen, Teknik Informatika, dan Rekayasa Komputer*, Vol. 24, No. 1, pp. 39-60, November, 2024.
This is an open access article under the CC BY-SA license (<https://creativecommons.org/licenses/by-sa/4.0/>)

Journal homepage: <https://journal.universitاسbumigora.ac.id/index.php/matrik>

1. INTRODUCTION

The majority of optimization issues related to next-generation networks have been resolved in the literature using centralized optimization techniques. Nevertheless, these methods rely on basic presumptions regarding the information needed to describe network situations. But these assumptions become unrealistic as mobile networking settings become more unpredictable [1]. Developing a distributed algorithm involves coming up with a method that can function on its own without centralized coordination or global knowledge [2]. By reducing the failure effect in the central station, distributed power management can increase reliability and prevent the bottleneck effect of centralized power control [3, 4]. The use of Distributed Power Control (DPC) algorithms in wireless communications is aimed at maximizing energy efficiency [5], as well as use in femtocell networks [6–8]. A femtocell is a small cellular network typically used in indoor environments [9]. Femtocell is used to enhance cellular network quality [10]. Femtocell has a typical transmission power of about 10-100 mW and a coverage radius of about 10-30 meters [11, 12]. Apart from their very useful advantages, femtocells have several challenges in carrying out their functions. One of the biggest problems in femtocells is when collaborating macrocells and femtocells overloop together; in other words, cross-tier interference occurs. To overcome this cross-tier interference problem, it is necessary to use open-loop and close-loop methods or use a power control algorithm to be able to adjust the power required in the femtocell network [13, 6]. Interference in femtocell networks is divided into two types, namely cross-tier and co-tier interference. Interference occurs due to the simultaneous use of communication channels. Interference can occur in the uplink or downlink direction [14]. In addition, the user's position affects the amount of interference produced, particularly the route gain from the user to the cell. When compared to users who are farther away, users who are closer to other cells will produce higher interference values [15].

Power control is used to enhance network performance. This notion is nearly identical to that of military networks' power efficiency, which is to aim for optimizing the use of power sources, extend battery life, and improve personnel comfort in the field [16]. There are two main types of power control in femtocell networks: Centralized Power Control (CPC) and Distributed Power Control (DPC) [10]. Distributed Power Control (DPC) is a method used to regulate the transmission power of devices within the network so that interference can be reduced and network performance can be improved. The distributed mechanism aims to reduce control complexity at the base station [17]. In Distributed Power Control (DPC), each user will update the power for himself continuously until it reaches a convergent condition. The previous Signal-to-Interference-plus-Noise Ratio (SINR) state and user power are used for power updates in the Distributed Power Control (DPC) system [18]. This research focuses on power control in the uplink communication direction (Uplink Power Control). Therefore, user transmit power adjustments are made to minimize interference. High interference due to uplink coverage areas can be constrained if user transmission power, which is the cause of interference, is not controlled [19, 20]. The greater the distance between stations and other cells, the lower the likelihood of interference, resulting in better transmission and less interference [15].

In this work, we studied the variation of the Distributed Power Control (DPC) method for user power treatment when user power exceeds the maximum power. The variations of Distributed Power Control (DPC) analyzed consist of Distributed Constrained Power Control (DCPC), Half Distributed Constrained Power Control (HDCPC), and Generalized Distributed Constrained Power Control (GDCPC). The need for user power treatment is related to interference mitigation caused by excess transmit power by each user when reaching a convergence condition. There are gaps that have not been resolved by previous research, namely in analyzing the convergence speed by each user in the Distributed Power Control (DPC) variation method. In addition, channel allocation variations are also made different for feasibility and convergence testing. The difference between this research and the previous one is that there is an additional number of users implementing the Distributed Power Control (DPC) variation method in this study. This is intended to ensure that the user power treatment method can be implemented in conditions with few or many users. The objectives and contribution of the research are providing the proposed method for using a variety of distributed power controls that are appropriate to the conditions of a co-tier femtocell network with distributed users. It is hoped that the contribution of this work can provide the best method for autonomous power management in distributed networks.

The rest of this paper is structured as follows. Section 2 presents the research method. This section provides the system model and variation of Distributed Power Control (DPC) methods. Furthermore, this section also describes the simulation parameters. Section 3 provides the result and discussion. At the end of Section 3 are performance comparisons of all variation Distributed Power Control (DPC) methods in terms of target SINR, user power, and convergence rate. Finally, Section 4 concludes the work, offering future research opportunities and areas of improvement.

2. RESEARCH METHOD

This research is a quantitative type of research and uses the Distributed Power Control (DPC) variation method with data generated based on the femtocell network scheme. Based on the research flowchart in Figure 1, it is explained that the power control process starts with initializing user power and determining the maximum user power. Data generation in this study includes 2 types,

namely user data and channel data. Data generation is carried out by initializing at the beginning of the program the number of users and the number of channels used. The position or distance of the user pair, namely the transmitter (Tx) and receiver (Rx), are distributed randomly but still within the range of the femtocell coverage area in the co-tier network topology. The user model in the femtocell network is a pair of femto user equipment (FUE) and femto access point (FAP). User data generation is related to the number of femtocells used in the network topology to be simulated. This is because the users used based on the co-tier network topology are in the form of user pairs, namely between the transmitter (Tx) in the form of one femto user equipment (FUE) and the receiver in the form of one femto access point (FAP).

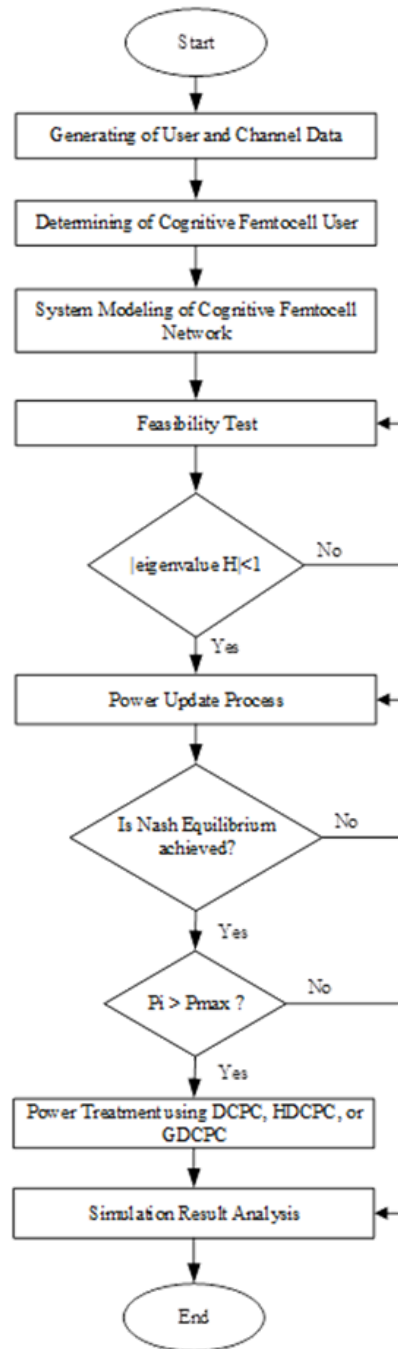


Figure 1. Flowchart of the Proposed System

As an initial stage, a feasibility test is carried out using the computation of the link gain matrix’s eigenvalue and the non-negative power vector calculation. The next stage is the power update process, which is also a convergence test, where if the Nash Equilibrium (NE) condition is achieved, then the system can be said to be converged. After the feasibility and convergence tests, the next stage is to test whether the user’s power usage exceeds the maximum power. If it exceeds the maximum power, power treatment will be carried out based on the proposed DPC variation method. The power update process will only be carried out if the user’s power is less than the maximum power using the DPC power update equation influenced by the target SINR, user SINR, and previous user power. This power update process will stop if the difference between the current and previous power is very small (approaching zero), which means that the convergence condition has been achieved.

2.1. System Model

In this study, the system model utilized depicts multiple Femtocell Access Points (FAP) as receivers at each node, along with Femtocell User Equipment (FUE) as transmitters, as shown in Figure 1. The system model comprises several adjacent femtocells, allowing each femtocell to transmit signals to Femtocell User Equipment (FUE). Figure 2 shows that the solid line indicates the desired signal while the dotted line indicates interference.

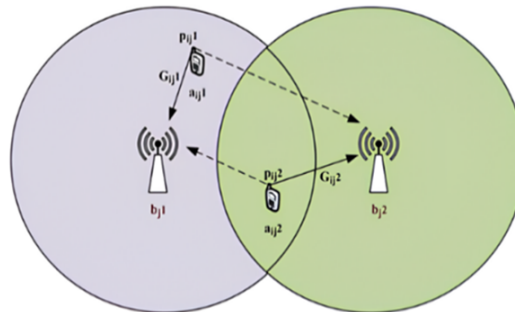


Figure 2. Femtocell network system model

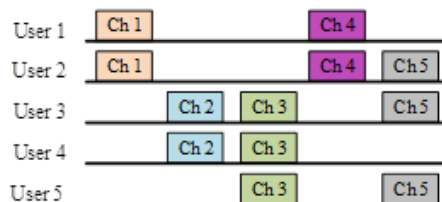


Figure 3. Channel scheme for 5 users

Channels from Figure 3, it can be observed that matrix H can be divided into 5 types according to the number of channels used. Matrix H1 represents the channel used by two users, User1 and User2, resulting in a size of 2×2 (corresponding to the number of users utilizing the channel). Users employing channel 1 also utilize channel 4, thus matrices H1 and H4 are identical. The remaining matrices H can be depicted as follows. The link gain matrix H can be differentiated based on users simultaneously utilizing channels. In Figure 4, it is evident that there are variations in the number of channels used by each user. Therefore, the link gain matrix H can be categorized into 10 types based on the number of channels utilized by each user. This link gain matrix H is generated from Equation 3.

$$H1=H4= \begin{bmatrix} h_{11} & h_{12} \\ h_{21} & h_{22} \end{bmatrix}$$

$$H2= \begin{bmatrix} h_{33} & h_{34} \\ h_{43} & h_{44} \end{bmatrix}$$

$$\mathbf{H3} = \begin{bmatrix} h_{33} & h_{34} & h_{35} \\ h_{43} & h_{44} & h_{45} \\ h_{53} & h_{54} & h_{55} \end{bmatrix}$$

$$\mathbf{H5} = \begin{bmatrix} h_{22} & h_{23} & h_{25} \\ h_{32} & h_{33} & h_{35} \\ h_{52} & h_{53} & h_{55} \end{bmatrix}$$

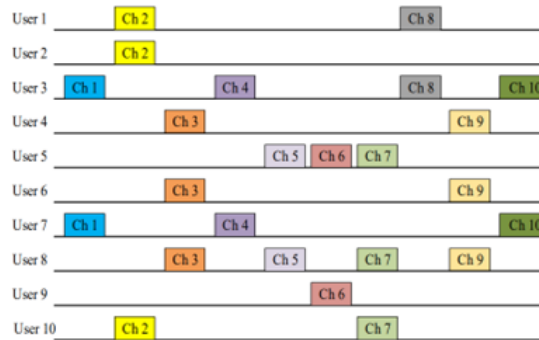


Figure 4. Channel scheme for 10 users

$$\mathbf{H1}=\mathbf{H4}=\mathbf{H10} = \begin{bmatrix} h_{33} & h_{37} \\ h_{73} & h_{77} \end{bmatrix}$$

$$\mathbf{H2} = \begin{bmatrix} h_{11} & h_{12} & h_{110} \\ h_{21} & h_{22} & h_{210} \\ h_{101} & h_{102} & h_{1010} \end{bmatrix}$$

$$\mathbf{H3}=\mathbf{H9} = \begin{bmatrix} h_{44} & h_{46} & h_{48} \\ h_{64} & h_{66} & h_{68} \\ h_{84} & h_{86} & h_{88} \end{bmatrix}$$

$$\mathbf{H5} = \begin{bmatrix} h_{55} & h_{58} \\ h_{85} & h_{88} \end{bmatrix}$$

$$\mathbf{H6} = \begin{bmatrix} h_{55} & h_{59} \\ h_{95} & h_{99} \end{bmatrix}$$

$$\mathbf{H7} = \begin{bmatrix} h_{55} & h_{58} & h_{510} \\ h_{85} & h_{88} & h_{810} \\ h_{105} & h_{108} & h_{1010} \end{bmatrix}$$

$$\mathbf{H8} = \begin{bmatrix} h_{11} & h_{13} \\ h_{31} & h_{33} \end{bmatrix}$$

2.2. Variation of Distributed Power Control (DPC)

Distributed power control schemes are simplified and arranged so that each station can effectively control power transmitted through the channels simultaneously. This helps improve overall energy control system efficiency and performance [5]. Several variations of Distributed Power Control (DPC) systems have been developed for co-tier femtocell networks, such as Distributed Constrained Power Control (DCPC), Half Distributed Constrained Power Control (HDCPC), and Generalized Distributed Constrained

Power Control (GDCPC) [21]. At the network's physical layer, power control methods are used to reduce the likelihood of interference in the network. However, to ensure the reliability of the power control system, all users must achieve the Signal-to-Interference-plus-Noise Ratio (SINR) value set as the appropriate standard, as shown in Equation 1 [21, 22]:

$$\gamma_i = \frac{p_i g_{ii}}{\sum_{i=1, i \neq j}^N p_{ij} g_{ij} + \sigma_0} \quad (1)$$

That is, the Signal-to-Interference-plus-Noise Ratio (SINR) formula with p_i representing the power of user i and p_{ij} denoting the power used by other users on the same channel and g_{ii} being the link gain of user i and g_{ij} is the link gain of a different user, and lastly σ_0 is noise [18]. To meet the criteria for a suitable distributed power control system, two requirements must be fulfilled: (a) the value of P^* must be a non-negative power vector, and (b) the absolute value of the link gain matrix must be $H < 1$ [21]. To meet the feasibility requirements, the following approach can be used as described in Equation 2 [21].

$$P^* = (I - H)^{-1} \eta \quad (2)$$

Notation P^* represents the total power used by users, while $H(h_{ij})$ is the normalized link gain matrix that can be determined using the following Equation (3) [21]. Meanwhile, η is a normalized noise vector that can be determined using equation 4 [21]. The values g_{ii} and g_{ij} represent the link gain values for user i and user j . The gain value for a user can be determined using Equation [18] 5. The link gain is a value influenced by the distance between users (d) and a constant path loss factor (α) equal to 4. Therefore, as the distance between users increases, the link gain value decreases due to increasing path loss. In Distributed Power Control (DPC), each user serves as a power controller for themselves and for other users. Each user continually adjusts the power used until reaching a converged state. The generation of new power is always linked to the previous power used by the user, and the Signal-to-Interference-plus-Noise Ratio (SINR) status and the power used by the user are utilized to update the power in the DPC system [21]. Distributed Power Control (DPC) has a power update formula that is shown in Equation 6.

$$h_{ij} = \gamma^{tar} \frac{g_{ij}}{g_{ii}} \quad (3)$$

$$\eta_i = \gamma^{tar} \frac{\sigma}{g_{ii}} \quad (4)$$

$$g_{ii} = \frac{A}{d^\alpha} \quad (5)$$

$$p_i^{(t+1)} = \frac{\gamma_i^{tar}}{\gamma_i^{(t)}} p_i^{(t)} \quad (6)$$

where γ_i^{tar} is the target Signal-to-Interference-plus-Noise Ratio (SINR), $\gamma_i^{(t)}$ is the Signal-to-Interference-plus-Noise Ratio (SINR) achieved by user i at time t and taken from Eq. 1, and $p_i^{(t+1)}$ is the power of the user after the iteration, with $p_i^{(t)}$ being the power of the user before the iteration. This method is known as the Power Balancing Algorithm (PBA) [21]:

Distributed Constrained Power Control (DCPC) is a power control method that considers the maximum power solution as a form of user power treatment. There are two conditions in the power iteration treatment, namely the first condition if $p_i^{(t+1)}$ after iteration, the power does not exceed or is equal to the maximum power, then the power after iteration does not need to be treated, but the second condition is if $p_i^{(t+1)}$ after iteration, the power exceeds the maximum power, then the power needs to be treated by making the power maximum power. Distributed Constrained Power Control (DCPC) has a power update formula that is shown in Equation 7:

$$p_i^{(t+1)} = \begin{cases} \frac{y_i^{tar}}{y_i^t} p_i^{(t)}, & \text{if } \frac{y_i^{tar}}{y_i^t} p_i^{(t)} \leq P_{max} \\ P_{max}, & \text{if } \frac{y_i^{tar}}{y_i^t} p_i^{(t)} > P_{max} \end{cases} \quad (7)$$

Generalized Distributed Constrained

Power Control (GDCPC) is a power control method that considers the user deactivation or to turn off the transmission power if the user's power after iteration exceeds the maximum power. GDCPC offers a more robust solution to the problem of excessive power. While this approach may seem more extreme, it helps ensure the network is not burdened by uncontrolled power usage, which

can cause interference. Generalized Distributed Constrained Power Control (GDCPC) has a power update formula that is shown in Equation 8.

$$p_i^{(t+1)} = \begin{cases} \frac{y_i^{tar}}{y_i} p_i^{(t)}, & \text{if } \frac{y_i^{tar}}{y_i} p_i^{(t)} \leq P_{max} \\ 0, & \text{if } \frac{y_i^{tar}}{y_i} p_i^{(t)} > P_{max} \end{cases} \quad (8)$$

To overcome the problems in the two previous methods (DCPC and GDCPC), a proposed method can be a solution for both methods by using half the maximum power, known as Half Distributed Constrained Power Control (HDCPC). This is intended so that users do not need to use maximum power continuously or stop transmitting data. Like DCPC, the Half Distributed Constrained Power Control (HDCPC) has a power update formula, as shown in Equation 9. Equation 6 is used to update the power (power update process) so that the user can achieve the target SINR with sufficient power and not exceed the maximum power or P_{max} , while Equations 7, 8, and 9 are used as power treatments in the form of DCPC, GDCPC, and HDCPC. All variations of power treatment are carried out if the power consumed by the user exceeds the maximum power Pmax.

$$p_i^{(t+1)} = \begin{cases} \frac{y_i^{tar}}{y_i} p_i^{(t)}, & \text{if } \frac{y_i^{tar}}{y_i} p_i^{(t)} \leq P_{max} \\ \frac{1}{2} P_{max}, & \text{if } \frac{y_i^{tar}}{y_i} p_i^{(t)} > P_{max} \end{cases} \quad (9)$$

2.3. Simulation Parameter

The simulation parameters used in this research are detailed in Table 1. The table includes parameters such as average noise level, target SINR, number of users, channels, maximum user power, and initial user power. The values for these parameters are specified as follows:

Table 1. Simulation Parameters

Parameters	Notations	Values
Average Noise Level	σ	10^{13} W
Target SINR	γ^{tar}	6.8 dB and 9.9 dB
Number of User	N	5 and 10
Number of Channel	K	5 and 10
Maximum User Power	P_{max}	50 mW
Initial User Power	P_{init}	2.22×10^{-16}

3. RESULT AND ANALYSIS

The findings of this research include scenarios of the number of users and user positions that produce feasible and non-feasible conditions. Fulfilling these feasible conditions is intended as an initial requirement for implementing the power control method so that the results will achieve the target SINR in convergent conditions (the Nash equilibrium condition is achieved). Therefore, this study also conducted feasibility tests and convergence tests. The application of this DPC variation method is intended to carry out a treatment process for users who use power exceeding the maximum permitted power. The treatment process is intended to avoid interference between users who use the channel simultaneously. The results of this research are in line with the research [23], where the use of Distributed Constrained Power Control (DCPC) and Deep Q-Network (DQN) methods both assume that the primary user and the secondary user work in a non-cooperative way. Comparing to the results of this research with the results of previous research which is using Deep Q-Network (DQN) method, the Distributed Constrained Power Control (DCPC) algorithm also requires a short iteration time to reach a convergent condition, with a value that is close to the optimal solution.

3.1. Network Topology

In the topology, as shown in Figure 5 below, a coverage radius of 260 m2 is utilized. The objective is to ensure that the distance between femtocells increases and that they do not interfere with each other, as the coverage radius of one femtocell is maximally 30 m. The coordinates of each Femtocell Access Points (FAP) and Femtocell User Equipment (FUE) in Figure 5 are outlined in Table 2. In the following semi-feasible topology shown in Figure 6, the radius distance is reduced to 100 square meters compared

to the feasible system. This reduction aims to allow for interference between femtocells or Femtocell Access Points (FAP). In a semi-feasible system, users have power exceeding the maximum power and fail to reach the Signal-to-Interference-plus-Noise Ratio (SINR) target.

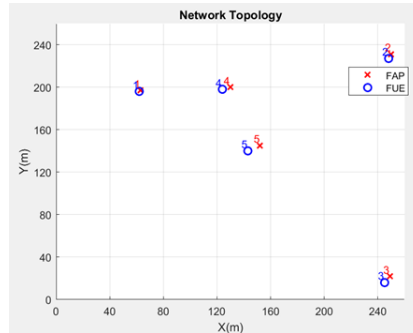


Figure 5. Feasible 5-user network topology

Table 2. Coordinates of feasible for 5 users

User	FAP		FUE	
	X (m)	Y (m)	X (m)	Y (m)
1	63	197	62	196
2	250	231	248	227
3	249	22	245	16
4	130	200	124	198
5	152	145	143	140

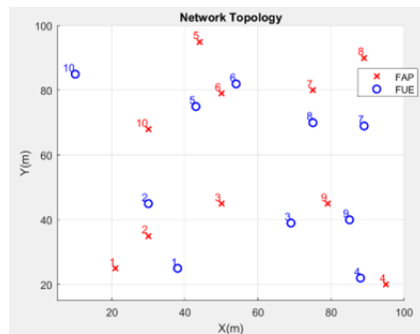


Figure 6. Semi-feasible 5-user network topology

The coordinates of each semi-feasible Femtocell Access Points (FAP) and Femtocell User Equipment (FUE) in Figure 6 are detailed in Table 3. Semi-feasible conditions can be achieved with a radius of 100 square meters for 10 users and 10 femtocells. Figure 7 below are the coordinates of each Femtocell Access Points (FAP) and Femtocell User Equipment (FUE) for the 10 semi-feasible users. The coordinates of each semi-feasible Femtocell Access Points (FAP) and Femtocell User Equipment (FUE) in Figure 7 are detailed in Table 4.

Table 3. Coordinates of semi-feasible for 5 users

User	FAP		FUE	
	X (m)	Y (m)	X (m)	Y (m)
1	29	45	40	45
2	38	75	29	69
3	51	57	56	46
4	50	98	50	80
5	65	72	78	88

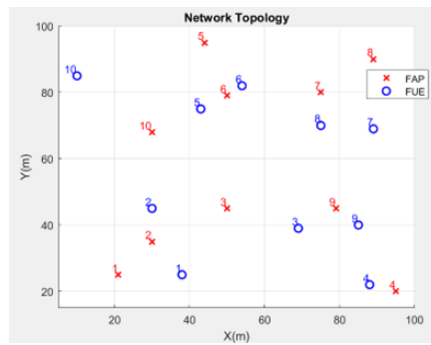


Figure 7. Semi-feasible 10-user network topology

Table 4. Coordinates of semi-feasible for 10 users

User	FAP		FUE	
	X (m)	Y (m)	X (m)	Y (m)
1	21	25	38	25
2	30	35	30	45
3	50	45	69	39
4	95	20	88	22
5	44	95	43	75
6	50	79	54	82
7	75	80	89	69
8	89	90	75	70
9	79	45	85	40
10	30	68	10	85

With a radius of 100 square meters for five users and five femtocells, a non-feasible condition may arise due to distant coordinates between Femtocell Access Points (FAP) and Femtocell User Equipment (FUE). Figure 8 below is a depiction of the coordinates for the Femtocell Access Points (FAP) and Femtocell User Equipment (FUE) of the five users in the non-feasible system.

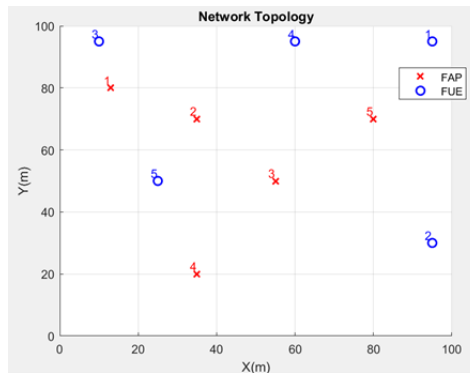


Figure 8. Non-feasible 5-user network topology

Table 5. Coordinates of non-feasible for 5 users

User	FAP		FUE	
	X (m)	Y (m)	X (m)	Y (m)
1	63	197	62	196
2	250	231	248	227
3	249	22	245	16
4	130	200	124	198
5	152	145	143	140

3.2. Feasible System

Based on the network topology for 5 users depicted in Figure 5 and the channel allocation shown in Figure 3, the eigenvalues for each matrix H can be computed. The absolute eigenvalues are calculated according to Eq. 3. Below are the values of matrix H and the eigenvalues for the feasible condition of 5 users:

$$\begin{aligned}
 H_1 &= \begin{bmatrix} h_{11} & h_{12} \\ h_{21} & h_{22} \end{bmatrix} = \begin{bmatrix} 0 & 0.0000000203396 \\ 0.0000022046327 & 0 \end{bmatrix} \\
 H_2 &= \begin{bmatrix} h_{33} & h_{34} \\ h_{43} & h_{44} \end{bmatrix} = \begin{bmatrix} 0 & 0.0000082951500 \\ 0.0000050100080 & 0 \end{bmatrix} \\
 H_3 &= \begin{bmatrix} h_{33} & h_{34} & h_{35} \\ h_{43} & h_{44} & h_{45} \\ h_{53} & h_{54} & h_{55} \end{bmatrix} = \begin{bmatrix} 0 & 0.0000082951500 & 0.0001206978043 \\ 0.0000050100080 & 0 & 0.0008427804660 \\ 0.0001206978043 & 0.0053785891115 & 0 \end{bmatrix} \\
 H_4 &= \begin{bmatrix} h_{11} & h_{12} \\ h_{21} & h_{22} \end{bmatrix} = \begin{bmatrix} 0 & 0.0000000203396 \\ 0.0000022046327 & 0 \end{bmatrix} \\
 H_5 &= \begin{bmatrix} h_{32} & h_{33} & h_{35} \\ h_{42} & h_{43} & h_{45} \\ h_{52} & h_{53} & h_{55} \end{bmatrix} = \begin{bmatrix} 0 & 0.0000085959153 & 0.0001206978043 \\ 0.000015400428 & 0 & 0.0000107051380 \\ 0.0001962756719 & 0.000287486822 & 0 \end{bmatrix} \\
 eigH_1 &= \begin{bmatrix} 0.000000211757756 \\ 0.000000211757756 \end{bmatrix} < 1 \\
 eigH_2 &= \begin{bmatrix} 0.00000644660902 \\ 0.00000644660902 \end{bmatrix} < 1 \\
 eigH_3 &= \begin{bmatrix} 0.002132955648088 \\ 0.002132054901974 \\ 0.000000900746114 \end{bmatrix} < 1 \\
 eigH_4 &= \begin{bmatrix} 0.000000211757756 \\ 0.000000211757756 \end{bmatrix} < 1 \\
 eigH_5 &= \begin{bmatrix} 0.000076441330181 \\ 0.000072888248355 \\ 0.000003553081826 \end{bmatrix} < 1
 \end{aligned}$$

Thus, it has been proven that the absolute value of the eigenvalue matrix H in the 5-user scheme with the researcher's chosen distance determination and channel allocation is less than 1. In other words, this fulfills one of the feasibility criteria. Another criterion for feasibility, besides the requirement that $|\text{eigenvalue matrix } H| < 1$, is the demonstration that the value of the power vector at convergence, denoted as P^* , is non-negative. This P^* value is obtained from Equation 2 using the notation in Eqs. 3, 4, and 5. Here are the power vector P^* values when reaching convergence in the 5-user scheme, while the power and Signal-to-Interference-plus-Noise Ratio (SINR) iterations are shown in Table 6 below.

$$\begin{aligned}
 P_1 &= \begin{bmatrix} 0.0000086014127 \\ 0.0008601395425 \end{bmatrix} W \\
 P_2 &= \begin{bmatrix} 0.0058145717195 \\ 0.0034405872253 \end{bmatrix} W \\
 P_3 &= \begin{bmatrix} 0.0058174904383 \\ 0.0034609662080 \\ 0.0241806364904 \end{bmatrix} W
 \end{aligned}$$

$$P_4 = \begin{bmatrix} 0.0000086014127 \\ 0.0008601395425 \end{bmatrix} W$$

$$P_5 = \begin{bmatrix} 0.0008604071389 \\ 0.0058152452064 \\ 0.0241621899813 \end{bmatrix} W$$

Table 6. Power and Signal-to-Interference-plus-Noise Ratio (SINR) iterations for the 5-user scheme

User(N)-Channel(M)	SINR Target 6.8 dB		SINR Target 9.9 dB	
	Power Iteration	SINR Iteration	Power Iteration	SINR Iteration
U1C2	8	8	7	8
U1C8	4	4	4	4
U2C2	6	7	7	7
U3C1	6	6	6	6
U3C4	6	6	6	6
U3C8	4	4	4	4
U3C10	6	6	6	6
U4C3	4	4	5	5
U4C9	4	4	5	5
U5C5	4	4	4	5
U5C6	4	4	4	5
U5C7	4	4	4	4
U6C3	4	4	5	5
U6C9	4	4	5	5
U7C1	5	6	6	6
U7C4	5	6	6	6
U7C10	5	6	6	6
U8C3	4	4	4	5
U8C5	4	4	4	4
U8C7	4	4	4	4
U8C9	4	4	4	5
U9C6	4	4	4	4
U10C2	7	8	8	8

3.3. Semi-Feasible System

We can determine the eigenvalues for each matrix H using the semi-feasible network topology for 5 users illustrated in Figure 7 and the channel allocation displayed in Figure 3. These eigenvalues are computed using Equation 3. The following provides the values of matrix H and the eigenvalues corresponding to the semi-feasible condition for 5 users:

$$H_1 = \begin{bmatrix} h_{11} & h_{12} \\ h_{21} & h_{22} \end{bmatrix} = \begin{bmatrix} 0 & 0.1218267875 \\ 0.2805664063 & 0 \end{bmatrix}$$

$$H_2 = \begin{bmatrix} h_{33} & h_{34} \\ h_{43} & h_{44} \end{bmatrix} = \begin{bmatrix} 0 & 0.0193069423 \\ 2.5412488430 & 0 \end{bmatrix}$$

$$H_3 = \begin{bmatrix} h_{33} & h_{34} & h_{35} \\ h_{43} & h_{44} & h_{45} \\ h_{53} & h_{54} & h_{55} \end{bmatrix} = \begin{bmatrix} 0 & 0.0193069423 & 0.4300444662 \\ 2.5412488430 & 0 & 8.5467942194 \\ 0.4300444662 & 1.5717455621 & 0 \end{bmatrix}$$

$$H_4 = \begin{bmatrix} h_{11} & h_{12} \\ h_{21} & h_{22} \end{bmatrix} = \begin{bmatrix} 0 & 0.1218267875 \\ 0.2805664063 & 0 \end{bmatrix}$$

$$H_5 = \begin{bmatrix} h_{22} & h_{23} & h_{25} \\ h_{32} & h_{33} & h_{35} \\ h_{52} & h_{53} & h_{55} \end{bmatrix} = \begin{bmatrix} 0 & 0.2360268165 & 0.0546587396 \\ 0.1067979149 & 0 & 0.2529431166 \\ 0.3924922692 & 0.4300444662 & 0 \end{bmatrix}$$

$$\text{eig}H_1 = \begin{bmatrix} 0.184879701319395 \\ 0.184879701319395 \end{bmatrix} < 1$$

$$\text{eig}H_2 = \begin{bmatrix} 0.221503374199453 \\ 0.221503374199453 \end{bmatrix} < 1$$

$$\text{eig}H_3 = \begin{bmatrix} 3.760718077032883 \\ 3.629683917154895 \\ 0.131034159877987 \end{bmatrix} < 1$$

$$\text{eig}H_4 = \begin{bmatrix} 0.184879701319395 \\ 0.184879701319395 \end{bmatrix} < 1$$

$$\text{eig}H_5 = \begin{bmatrix} 0.460224616823881 \\ 0.230112308411941 \\ 0.230112308411941 \end{bmatrix} < 1$$

The results above show that channels one, two, four, and five have satisfied the feasibility requirement, namely that the absolute eigenvalue values of matrix H are less than one. However, channel three does not meet the requirement as the absolute eigenvalue value of matrix H is not less than one, indicating that this scheme demonstrates semi-feasibility. In addition to the condition that the absolute eigenvalue values of matrix H must be below one, another feasibility requirement is that the power vector values must be non-negative. The power vector values are obtained from the matrix values calculated using the power vector formula in Eq. 2, which involves subtracting the identity matrix from the inverted matrix H and multiplying it by the user's noise.

$$P_1 = \begin{bmatrix} 0.0363104758 \\ 0.0396236245 \end{bmatrix} W$$

$$P_2 = \begin{bmatrix} 0.0527849137 \\ 0.3598746174 \end{bmatrix} W$$

$$P_3 = \begin{bmatrix} 0.0125792297 \\ -0.2914386779 \\ -0.0642510669 \end{bmatrix} W$$

$$P_4 = \begin{bmatrix} 0.0363104758 \\ 0.0396236245 \end{bmatrix} W$$

$$P_5 = \begin{bmatrix} 0.1008386283 \\ 0.1849840559 \\ 0.5075365052 \end{bmatrix} W$$

The test results of the power vector values above using the multichannel multiuser scheme indicate that channel three has negative values, indicating semi-feasibility, as the other channels meet the feasibility criteria. From the above 10-user model system, the following matrix H is obtained using Equation 3 to find its eigenvalues.

$$H_1 = H_4 = H_{10} = \begin{bmatrix} h_{33} & h_{37} \\ h_{73} & h_{77} \end{bmatrix} = \begin{bmatrix} 0 & 0.3635376001 \\ 0.1553926869 & 0 \end{bmatrix}$$

$$H_2 = \begin{bmatrix} h_{11} & h_{12} & h_{110} \\ h_{21} & h_{22} & h_{210} \\ h_{101} & h_{102} & h_{1010} \end{bmatrix} = \begin{bmatrix} 0 & 21.1162552052 & 0.1551939040 \\ 0.2939129758 & 0 & 0.2429951294 \\ 0.2331460256 & 0.3838409988 & 0 \end{bmatrix}$$

$$H_3 = H_9 = \begin{bmatrix} h_{44} & h_{46} & h_{48} \\ h_{64} & h_{66} & h_{68} \\ h_{84} & h_{86} & h_{88} \end{bmatrix} = \begin{bmatrix} 0 & 0.0008672804 & 0.0008929706 \\ 0.0001392273 & 0 & 0.0025578973 \\ 0.2872138882 & 4.8460961889 & 0 \end{bmatrix}$$

$$\begin{aligned}
H_5 &= \begin{bmatrix} h_{55} & h_{58} \\ h_{85} & h_{88} \end{bmatrix} = \begin{bmatrix} 0 & 0.1995238565 \\ 0.9602737700 & 0 \end{bmatrix} \\
H_6 &= \begin{bmatrix} h_{55} & h_{59} \\ h_{95} & h_{99} \end{bmatrix} = \begin{bmatrix} 0 & 0.2267425291 \\ 0.0011425224 & 0 \end{bmatrix} \\
H_7 &= \begin{bmatrix} h_{55} & h_{58} & h_{510} \\ h_{85} & h_{88} & h_{810} \\ h_{105} & h_{108} & h_{1010} \end{bmatrix} = \begin{bmatrix} 0 & 0.1995238565 & 23.0083073815 \\ 0.9602737700 & 0 & 0.5867287078 \\ 2.0462942209 & 0.0822179370 & 0 \end{bmatrix} \\
H_8 &= \begin{bmatrix} h_{11} & h_{13} \\ h_{31} & h_{33} \end{bmatrix} = \begin{bmatrix} 0 & 1.9191406250 \\ 0.1714785920 & 0 \end{bmatrix} \\
eigH_1 = eigH_4 = eigH_{10} &= \begin{bmatrix} 0.460224616823881 \\ 0.230112308411941 \\ 0.230112308411941 \end{bmatrix} < 1 \\
eigH_2 &= \begin{bmatrix} 2.607916869816015 \\ 2.415206805119064 \\ 0.192710064696951 \end{bmatrix} < 1 \\
eigH_3 = eigH_9 &= \begin{bmatrix} 0.112531891893593 \\ 0.112433914082086 \\ 0.000097977811507 \end{bmatrix} < 1 \\
eigH_5 &= \begin{bmatrix} 0.437718546427032 \\ 0.437718546427032 \end{bmatrix} < 1 \\
eigH_6 &= \begin{bmatrix} 0.016095291812496 \\ 0.016095291812496 \end{bmatrix} < 1 \\
eigH_7 &= \begin{bmatrix} 6.90069263681305 \\ 6.857241448352568 \\ 0.043451188460481 \end{bmatrix} < 1 \\
eigH_8 &= \begin{bmatrix} 0.573665 \\ 0.573665 \end{bmatrix} < 1
\end{aligned}$$

From the obtained results, the eigenvalue values of matrix H are partially less than one and partially greater than one. Where the feasibility criterion states that the absolute eigenvalue values of the matrix should be below one, this system is considered semi-feasible. The matrices that meet the feasibility criteria are matrices one, four, ten, three, nine, five, six, and eight. Meanwhile, the matrices that do not meet the feasibility criteria, as the absolute eigenvalue values of matrix H are less than one, are matrices two and seven. Therefore, this scheme can be classified as a semi-feasible system. One of the feasibility criteria is that the power vector values are nonnegative when the power values before treatment have reached convergence or do not exceed the maximum power. Below are the power vector values for the multiuser multichannel 10-user scheme.

$$\begin{aligned}
P_1 = P_4 = P_{10} &= \begin{bmatrix} 0.4424651960 \\ 0.2848422571 \end{bmatrix} W \\
P_2 &= \begin{bmatrix} -0.9183113889 \\ -0.0577596356 \\ 0.7845445701 \end{bmatrix} W \\
P_3 = P_9 &= \begin{bmatrix} 0.0067415210 \\ 0.0033451451 \\ 0.7819854557 \end{bmatrix} W
\end{aligned}$$

$$P_5 = \begin{bmatrix} 0.6162551683 \\ 1.3556119762 \end{bmatrix} W$$

$$P_6 = \begin{bmatrix} 0.3476825775 \\ 0.0083986831 \end{bmatrix} W$$

$$P_7 = \begin{bmatrix} -0.5277885514 \\ 0.2335518937 \\ -0.0399927709 \end{bmatrix} W$$

$$P_8 = \begin{bmatrix} 1.2371635969 \\ 0.5510613971 \end{bmatrix} W$$

From the results above, it can be observed that some power vectors for certain channels are non-negative, while others are negative. This indicates that the scheme is semi-feasible. The nonnegative power vectors are vectors one, four, ten, three, nine, five, six, and eight. Meanwhile, the negative power vectors are found in vectors two and seven. This also proves that if the requirement for the absolute eigenvalue values is not met, the condition for nonnegative power vectors will also not be fulfilled. After conducting the feasibility test, the next step is to test the convergence of power and Signal-to-Interference-plus-Noise Ratio (SINR) in the semi-feasible multichannel multiuser scheme. They are shown in Figures 9 and 10 below.

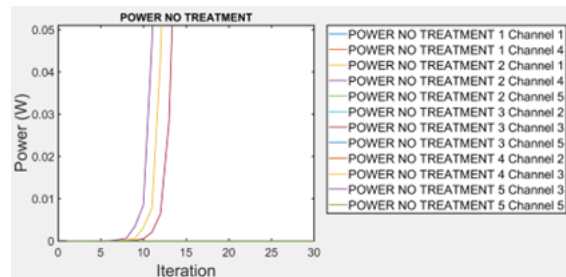


Figure 9. Power of the 5-user scheme

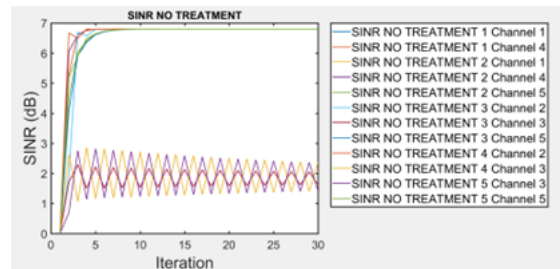


Figure 10. Signal-to-Interference-plus-Noise Ratio (SINR) target 6.8 dB for 5 users

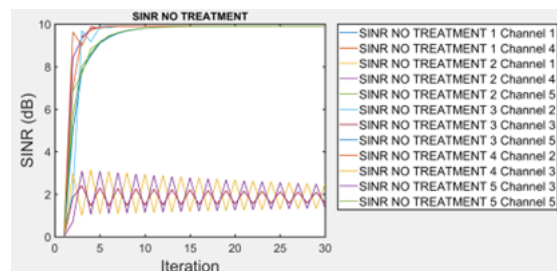


Figure 11. Signal-to-Interference-plus-Noise Ratio (SINR) target 9.9 dB for 5 users

Figure 11 depicts several users that fail to converge below the maximum power of 0.05W due to a reduction in their coverage area by 100 square meters, resulting in interference that prolongs the convergence iterations. In Figure 12, three users experience continuously increasing power levels, exceeding the maximum power limit of 50mW. These users are all located in channel three, consequently affecting the Signal-to-Interference-plus-Noise Ratio (SINR). None of the users in channel three achieved the Signal-to-Interference-plus-Noise Ratio (SINR) targets of 6.8 dB and 9.9 dB. This is further illustrated in Figures 13 and 14.

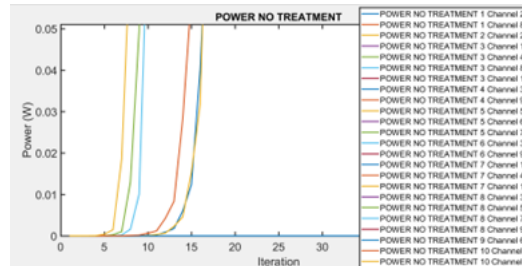


Figure 12. Power of the 10-user scheme

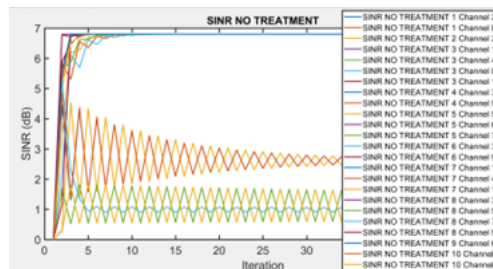


Figure 13. Signal-to-Interference-plus-Noise Ratio (SINR) target 6.8 dB for 10 users

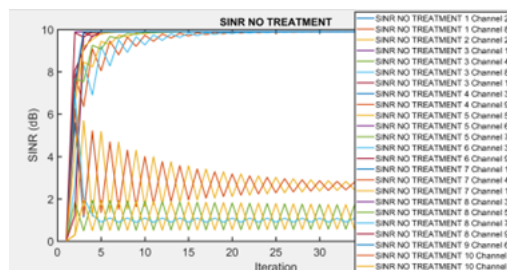


Figure 14. Signal-to-Interference-plus-Noise Ratio (SINR) target 9.9 dB for 10 users

By introducing variations to some users that do not meet the feasibility requirements in the semi-feasible system, Distributed Constrained Power Control (DCPC) variation limits the power to the maximum power of 0.05W, Half Distributed Constrained Power Control (HDCPC) variation reduces the power to half of the maximum power of 0.025W, and Generalized Distributed Constrained Power Control (GDCPC) variation halts the user’s transmission by setting the power to 0, and it will resume if the power does not exceed the maximum power by adjusting the positions of Femtocell Access Points (FAP) and Femtocell User Equipment (FUE).

In Tables 7 and 8, the Signal-to-Interference-plus-Noise Ratio (SINR) always converges after the treatment process with DPC variations. However, the resulting SINR from the variation treatment does not always meet the Signal-to-Interference-plus-Noise Ratio (SINR) target; some improve upon the Signal-to-Interference-plus-Noise Ratio (SINR) target while others do not. Table 9 presents the number of iterations required to achieve the Signal-to-Interference-plus-Noise Ratio (SINR) convergence. For Distributed Constrained Power Control (DCPC) and Half Distributed Constrained Power Control (HDCPC), convergence occurs at the same iteration, except for Generalized Distributed Constrained Power Control (GDCPC).

Table 7. Impact of variations on the Signal-to-Interference-plus-Noise Ratio (SINR) 6.8 dB for 5 users

User-Channel	SINR Before (dB)	SINR After (dB)		
		DCPC	HDCPC	GDCPC
U1C1	6.8	6.8	6.8	6.8
U1C4	6.8	6.8	6.8	6.8
U2C1	6.8	6.8	6.8	6.8
U2C4	6.8	6.8	6.8	6.8
U2C5	6.8	6.8	6.8	6.8
U3C2	6.8	6.8	6.8	6.8
U3C3	1.69483	11.99788	11.99787	0
U3C5	6.8	6.8	6.8	6.8
U4C2	6.8	6.8	6.8	6.8
U4C3	2.15642	6.74232	6.74231	0
U5C3	1.54911	0.40357	0.40357	0
U5C5	6.8	6.8	6.8	6.8

Table 8. Impact of variations on the Signal-to-Interference-plus-Noise Ratio (SINR) 9.9 dB for 5 users

User-Channel	SINR Before (dB)	SINR After (dB)		
		DCPC	HDCPC	GDCPC
U1C1	9.9	9.9	9.9	9.9
U1C4	9.9	9.9	9.9	9.9
U2C1	9.9	9.9	9.9	9.9
U2C4	9.9	9.9	9.9	9.9
U2C5	9.9	9.9	9.9	9.9
U3C2	9.9	9.9	9.9	9.9
U3C3	1.67043	11.99788	11.99787	0
U3C5	9.9	9.9	9.9	9.9
U4C2	9.9	9.9	9.9	9.9
U4C3	2.22825	6.74232	6.74231	0
U5C3	1.49992	0.40357	0.40357	0
U5C5	9.9	9.9	9.9	9.9

Table 9. Convergence iterations for 5 users

User-Channel	Iteration (Before)	Iteration (After)		
		DCPC	HDCPC	GDCPC
U1C1	17	17	17	17
U1C4	17	17	17	17
U2C1	16	16	16	16
U2C4	16	16	16	16
U2C5	34	34	34	34
U3C2	19	19	19	19
U3C3	not convergent	14	14	14
U3C5	34	34	34	34
U4C2	18	18	18	18
U4C3	not convergent	14	14	13
U5C3	not convergent	14	14	12
U5C5	34	34	34	34

Tables 10 and 11 present the results of the Signal-to-Interference-plus-Noise Ratio (SINR) influenced by the Signal-to-Interference-plus-Noise Ratio (SINR) variations of 6.8 dB and 9.9 dB. Among the three variations, it is observed that Distributed Constrained Power Control (DCPC) and Half Distributed Constrained Power Control (HDCPC) yield nearly identical SINR results. However, Distributed Constrained Power Control (DCPC) slightly outperforms Half Distributed Constrained Power Control (HDCPC) but consumes more power. Generalized Distributed Constrained Power Control (GDCPC), under certain conditions, needs to shut down power to stop data transmission, resulting in the Signal-to-Interference-plus-Noise Ratio (SINR) dropping to zero.

Table 10. Impact of variations on the Signal-to-Interference-plus-Noise Ratio (SINR) 6.8 dB for 10 users

User-Channel	SINR Before (dB)	SINR After (dB)		
		DCPC	HDCPC	GDCPC
U1C2	2.64664	2.72456	2.72456	0
U1C8	6.8	6.8	6.8	6.8
U2C2	2.56574	2.68102	2.68102	0
U3C1	6.8	6.8	6.8	6.8
U3C4	6.8	6.8	6.8	6.8
U3C8	6.8	6.8	6.8	6.8
U3C10	6.8	6.8	6.8	6.8
U4C3	6.8	6.8	6.8	6.8
U4C9	6.8	6.8	6.8	6.8
U5C5	6.8	6.8	6.8	6.8
U5C6	6.8	6.8	6.8	6.8
U5C7	1.54827	6.02922	6.02921	0
U6C3	6.8	6.8	6.8	6.8
U6C9	6.8	6.8	6.8	6.8
U7C1	6.8	6.8	6.8	6.8
U7C4	6.8	6.8	6.8	6.8
U7C10	6.8	6.8	6.8	6.8
U8C3	6.8	6.8	6.8	6.8
U8C5	6.8	6.8	6.8	6.8
U8C7	1.05912	13.53821	13.53808	0
U8C9	6.8	6.8	6.8	6.8
U9C6	6.8	6.8	6.8	6.8
U10C2	2.64680	0.54761	0.54760	0
U10C7	0.62533	0.09896	0.09896	0

Table 11. Impact of variations on the Signal-to-Interference-plus-Noise Ratio (SINR) 9,9 dB for 10 users

User-Channel	SINR Before (dB)	SINR After (dB)		
		DCPC	HDCPC	GDCPC
U1C2	2.65912	2.72456	2.72456	0
U1C8	9.9	9.9	9.9	9.9
U2C2	2.55272	2.68102	2.68102	0
U3C1	9.9	9.9	9.9	9.9
U3C4	9.9	9.9	9.9	9.9
U3C8	9.9	9.9	9.9	9.9
U3C10	9.9	9.9	9.9	9.9
U4C3	9.9	9.9	9.9	9.9
U4C9	9.9	9.9	9.9	9.9
U5C5	9.9	9.9	9.9	9.9
U5C6	9.9	9.9	9.9	9.9
U5C7	1.62023	6.02922	6.02921	0
U6C3	9.9	9.9	9.9	9.9
U6C9	9.9	9.9	9.9	9.9
U7C1	9.9	9.9	9.9	9.9
U7C4	9.9	9.9	9.9	9.9
U7C10	9.9	9.9	9.9	9.9
U8C3	9.9	9.9	9.9	9.9
U8C5	9.9	9.9	9.9	9.9
U8C7	1.06655	13.53821	13.53808	0
U8C9	9.9	9.9	9.9	9.9
U9C6	9.9	9.9	9.9	9.9
U10C2	2.65933	0.54761	0.54760	0
U10C7	0.59732	0.09896	0.09896	0

Table 12. Convergence iterations for 10 users

User-Channel	Iteration (Before)	Iteration (After)		
		DCPC	HDCPC	GDCPC
U1C2	not convergent	17	17	17
U1C8	42	46	46	46
U2C2	not convergent	17	17	17
U3C1	18	19	19	19
U3C4	18	19	19	19
U3C8	43	47	47	47
U3C10	18	19	19	19
U4C3	11	13	13	13
U4C9	11	13	13	13
U5C5	29	31	31	31
U5C6	7	8	8	8
U5C7	not convergent	10	10	10
U6C3	13	13	13	13
U6C9	13	13	13	13
U7C1	17	19	19	19
U7C4	17	19	19	19
U7C10	17	19	19	19
U8C3	12	12	12	12
U8C5	28	32	32	32
U8C7	not convergent	10	10	10
U8C9	12	12	12	12
U9C6	7	8	8	8
U10C2	not convergent	17	17	17
U10C7	not convergent	10	10	10

However, this can be overcome by adjusting the power so that it does not exceed the maximum or by changing the distance to avoid interference. Although the Signal-to-Interference-plus-Noise Ratio (SINR) results of various treatment variations do not all meet the target, stable or converging Signal-to-Interference-plus-Noise Ratio (SINR) is considered adequate for data transmission. The differences in Signal-to-Interference-plus-Noise Ratio (SINR) results among users after treatment variations occur due to the number of users using the same channel. Table 12 indicates the number of iterations required to achieve SINR convergence, which is the same for Distributed Constrained Power Control (DCPC), Half Distributed Constrained Power Control (HDCPC), and Generalized Distributed Constrained Power Control (GDCPC).

3.4. Non-Feasible System

Based on the non-feasible network topology for 5 users depicted in Figure 8 and the channel allocation shown in Figure 3, the eigenvalues for each matrix H can be computed. The following matrix H is used in the scheme for non-feasible 5 users and is obtained by using Equation 3. Considering the distance between user positions and the utilization of channels used by the 5 users in the non-feasible system.

$$H_1 = \begin{bmatrix} h_{11} & h_{12} \\ h_{21} & h_{22} \end{bmatrix} = \begin{bmatrix} 0 & 18.3950134407 \\ 2.1611106890 & 0 \end{bmatrix}$$

$$H_2 = \begin{bmatrix} h_{33} & h_{34} \\ h_{43} & h_{44} \end{bmatrix} = \begin{bmatrix} 0 & 2.8553472000 \\ 63.2064247472 & 0 \end{bmatrix}$$

$$H_3 = \begin{bmatrix} h_{33} & h_{34} & h_{35} \\ h_{43} & h_{44} & h_{45} \\ h_{53} & h_{54} & h_{55} \end{bmatrix} = \begin{bmatrix} 0 & 2.8553472000 & 98.4793209877 \\ 63.2064247472 & 0 & 252.8256989887 \\ 98.4793209877 & 79.7682500000 & 0 \end{bmatrix}$$

It is stated that channel 1 is utilized by 2 users, channel 2 by 2 users, channel 3 by 3 users, channel 4 by 2 users, and channel 5 by 3 users. This is the scheme for 5 users in the utilized channels to calculate the eigenvalue of matrix H. As one of the feasibility conditions is $|\text{eigenvalue of matrix } H| < 1$, here are the eigenvalues of the non-feasible scheme for 5 users.

$$\text{eig}H_1 = \begin{bmatrix} 6.305050370218737 \\ 6.305050370218737 \end{bmatrix}$$

$$eigH_2 = \begin{bmatrix} 13.434146341466146 \\ 13.434146341466146 \end{bmatrix}$$

$$eigH_3 = \begin{bmatrix} 182.107192131157642 \\ 162.983036797847649 \\ 19.124155333309993 \end{bmatrix}$$

$$eigH_4 = \begin{bmatrix} 6.305050370218737 \\ 6.305050370218737 \end{bmatrix}$$

$$eigH_5 = \begin{bmatrix} 155.245451038304947 \\ 134.016195544595532 \\ 21.229255493709416 \end{bmatrix}$$

Hence, it has been proven that the absolute value of the eigenvalue of matrix H in the scheme for 5 users, with the determination of distance and channel utilization used by the researcher, exceeds 1. In other words, this fails to meet one of the feasibility conditions. Another condition for feasibility, besides the requirement that $|\text{eigenvalue of matrix } H| < 1$, is the demonstration of non-negative values for the power vector. Below are the power vector values in the 5-user scheme:

$$P_1 = \begin{bmatrix} -30.2790324784 \\ -7.2909089496 \end{bmatrix} W$$

$$P_2 = \begin{bmatrix} -1.5328740895 \\ -12.8894904367 \end{bmatrix} W$$

$$P_3 = \begin{bmatrix} 0.0510510867 \\ -0.3835978433 \\ -0.3465168107 \end{bmatrix} W$$

$$P_4 = \begin{bmatrix} -30.2790324784 \\ -7.2909089496 \end{bmatrix} W$$

$$P_5 = \begin{bmatrix} -0.3848125495 \\ 0.9716668147 \\ -1.8692709760 \end{bmatrix} W$$

From the calculation results of the power vector conducted with the scheme of five users, considering the distance between users, the distance between Femtocell Access Points (FAPs), the distance between users and Femtocell Access Points (FAPs), and considering the usage of users on channels, it is found that the power vector values are negative for all channels. This does not meet the second feasibility condition, namely the non-negative power vector value requirement. Therefore, it can be concluded that the scheme for 5 users with the target Signal-to-Interference-plus-Noise Ratio (SINR) of 6.8 dB does not satisfy both conditions considered feasible.

3.5. Discussion

This research begins by creating user and channel data for the scheme, namely 5 users and 10 users, with predetermined channel allocation. The simulation begins by simulating users' location in the femtocell network, which is made randomly and distinguished in 2 different conditions, namely feasible and infeasible users, through a feasibility test. Model validation is carried out using a feasibility test and a convergence test. The feasibility test is related to the user gain, which in this case is influenced by the distance of the femtocell user equipment (FUE) to the femtocell access point (FAP) and also the use of channels by each user through the calculation of the absolute value of the eigenvalue of the link gain matrix H which is less than 1 ($|\text{eigenvalue of matrix } H| < 1$). If it meets the requirements, the system will continue with the next feasibility test, namely the calculation of the non-negative power vector value, which means that the resulting power value is positive, and this means that the value is feasible. Basically, if the eigenvalue meets the requirements, the power vector value will also be obtained as a non-negative (positive) result. The next model validation uses a convergence test where if the feasibility test has been met, the system will reach a convergent condition (Nash Equilibrium) at

a certain Signal-to-Interference-plus-Noise Ratio (SINR) or power value. Ideally, the Signal-to-Interference-plus-Noise Ratio (SINR) value obtained during the convergent condition can reach the specified target Signal-to-Interference-plus-Noise Ratio (SINR) with a power value below the maximum power. The use of Distributed Power Control (DPC) variations in this study is intended for power treatment when the user's power exceeds the maximum power allowed, namely by making the power exactly at the maximum power (in Distributed Constrained Power Control), or the power is made zero or the transmission process is turned off (in Generalized Distributed Constrained Power Control), or the power is made half the maximum power (in Half Distributed Constrained Power Control).

4. CONCLUSION

The Distributed Power Control (DPC) system generates feasible, semi-feasible, and non-feasible conditions based on distance and channel utilization. When a system has a non-negative power vector and an absolute eigenvalue of $H < 1$, it meets the requirements for feasibility. When some users meet the feasibility requirements while others do not, the system is said to be semi-feasible. In contrast, a non-feasible system completely fails to satisfy the requirements for feasibility. The power and the Signal-to-Interference-plus-Noise Ratio (SINR) criteria of semi-feasible systems are invariably changed by variations of Distributed Power Control (DPC), namely Distributed Constrained Power Control (DCPC), Half Distributed Constrained Power Control (HDCPC), and Generalized Distributed Constrained Power Control (GDCPC), from non-convergent to convergent below or equal to the maximum power and modify the Signal-to-Interference-plus-Noise Ratio (SINR) to converge. Since Half Distributed Constrained Power Control (HDCPC) uses power more wisely and produces almost the same Signal-to-Interference-plus-Noise Ratio (SINR) as Distributed Constrained Power Control (DCPC), it can be concluded that the Half Distributed Constrained Power Control (HDCPC) is more effective than Distributed Constrained Power Control (DCPC). Compared to Generalized Distributed Constrained Power Control (GDCPC), Half Distributed Constrained Power Control (HDCPC) is simpler to construct since it does not call for deactivating users or halting transmission when the maximum power is exceeded. It can be concluded that to answer the problem of power treatment needs, in conditions where the user uses power that exceeds the maximum power, a treatment process is needed using the DPC variation method. The results show that all methods are able to provide power treatment solutions. However, the only one that is ideal and can still maintain communication is the Half Distributed Constrained Power Control (HDCPC) power treatment.

Further research involves applying the game theory method to the self-organized power control system in co-tier and cross-tier femtocell networks. In addition, implementing user power treatment is still needed if the user who reaches convergence has the user power above the maximum power using the deep learning method.

5. ACKNOWLEDGEMENTS

This research is supported by the Digital Engineering Laboratory, Institut Teknologi Telkom Purwokerto. The all authors extend gratitude to all parties involved in this research.

6. DECLARATIONS

AUTHOR CONTRIBUTION

The author's contributions are elaborated as follows: Fatur Rahman Harahap focused on software programming and visualization; Anggun Fitriani Isnawati coordinated the research, including conceptualization, methodology, resources, validation, analysis, and supervision; Khoirun Ni'amah did the writing, review, administration, and editing.

FUNDING STATEMENT

This research is funded by the Institute of Research and Community Services (LPPM), Institut Teknologi Telkom Purwokerto.

REFERENCES

- [1] Z. Xiong, Y. Zhang, D. Niyato, R. Deng, P. Wang, and L.-C. Wang, "Deep Reinforcement Learning for Mobile 5G and Beyond: Fundamentals, Applications, and Challenges," *IEEE Vehicular Technology Magazine*, vol. 14, no. 2, pp. 44–52, Jun. 2019, <https://doi.org/10.1109/MVT.2019.2903655>.
- [2] A. Nedić and J. Liu, "Distributed Optimization for Control," *Annual Review of Control, Robotics, and Autonomous Systems*, vol. 1, no. 1, pp. 77–103, May 2018, <https://doi.org/10.1146/annurev-control-060117-105131>.
- [3] H. Hua, Z. Wei, Y. Qin, T. Wang, L. Li, and J. Cao, "Review of distributed control and optimization in energy internet: From

- traditional methods to artificial intelligence-based methods,” *IET Cyber-Physical Systems: Theory & Applications*, vol. 6, no. 2, pp. 63–79, Jun. 2021, <https://doi.org/10.1049/cps2.12007>.
- [4] S. Najeh and A. Bouallegue, “Distributed vs centralized game theory-based mode selection and power control for D2D communications,” *Physical Communication*, vol. 38, p. 100962, Feb. 2020, <https://doi.org/10.1016/j.phycom.2019.100962>.
- [5] R. Aslani and M. Rasti, “A Distributed Power Control Algorithm for Energy Efficiency Maximization in Wireless Cellular Networks,” *IEEE Wireless Communications Letters*, vol. 9, no. 11, pp. 1975–1979, Nov. 2020, <https://doi.org/10.1109/LWC.2020.3010156>.
- [6] Y. Liu, L. Hao, Z. Liu, K. Sharif, Y. Wang, and S. K. Das, “Mitigating Interference via Power Control for Two-Tier Femtocell Networks: A Hierarchical Game Approach,” *IEEE Transactions on Vehicular Technology*, vol. 68, no. 7, pp. 7194–7198, Jul. 2019, <https://doi.org/10.1109/TVT.2019.2916715>.
- [7] O. Sevim, H. Y. Oksuz, and M. Akar, “Joint Frequency and Power Control for Self-Organizing OFDMA Femtocell Networks,” *IEEE Transactions on Vehicular Technology*, vol. 69, no. 5, pp. 5089–5101, May 2020, <https://doi.org/10.1109/TVT.2020.2978945>.
- [8] Z. Li, Z. Li, and Z. Ding, “Distributed Generalized Nash Equilibrium Seeking and Its Application to Femtocell Networks,” *IEEE Transactions on Cybernetics*, vol. 52, no. 4, pp. 2505–2517, Apr. 2022, <https://doi.org/10.1109/TCYB.2020.3004635>.
- [9] S. Alotaibi, “Femtocell Networks Interference Management Approaches,” *International Journal of Computer Science and Network Security*, vol. 22, no. 4, pp. 329–339, Apr. 2022, <https://doi.org/10.22937/IJCSNS.2022.22.4.39>.
- [10] A. Isnawati, J. Hendry, and E. Cahyadi, “Coverage Planning for Co-tier Femtocell Networks Using Voronoi Diagram and Gradient-based Optimization Method,” *International Journal of Intelligent Engineering and Systems*, vol. 13, no. 4, pp. 389–398, Aug. 2020, <https://doi.org/10.22266/ijies2020.0831.34>.
- [11] S. Alotaibi, “Radio Resource Scheduling Approach For Femtocell Networks,” *International Journal of Computer Science and Network Security*, vol. 22, no. 4, pp. 394–400, Apr. 2022, <https://doi.org/10.22937/IJCSNS.2022.22.4.46>.
- [12] M. S. Al-omari, M. A. Alomari, A. R. Ramli, A. Sali, R. S. Azmir, and M. H. Yusoff, “Effects of Femtocell Ultradense Deployment on Downlink Performance in LTE Heterogeneous Networks,” *Wireless Communications and Mobile Computing*, vol. 2021, no. 1, p. 2735935, Jan. 2021, <https://doi.org/10.1155/2021/2735935>.
- [13] T. U. Hassan and F. Gao, “An Active Power Control Technique for Downlink Interference Management in a Two-Tier Macro-Femto Network,” *Sensors*, vol. 19, no. 9, p. 2015, Apr. 2019, <https://doi.org/10.3390/s19092015>.
- [14] R. Aljjakli and K. Abdullah, “Cross-Tier Interference Avoidance Technique for LTE-A Femtocell Networks Using Fractional Frequency Reuse,” in *2020 IEEE 5th International Symposium on Telecommunication Technologies (ISTT)*. Shah Alam, Malaysia: IEEE, Nov. 2020, pp. 117–122, <https://doi.org/10.1109/ISTT50966.2020.9279383>.
- [15] R. Nikbakht, R. Mosayebi, and A. Lozano, “Uplink Fractional Power Control and Downlink Power Allocation for Cell-Free Networks,” *IEEE Wireless Communications Letters*, vol. 9, no. 6, pp. 774–777, Jun. 2020, <https://doi.org/10.1109/LWC.2020.2969404>.
- [16] D. Widiatmoko, A. Aripriharta, K. Kasiyanto, D. Irmanto, and M. Wahyu Prasetyo, “Power Efficiency using Bank Capacitor Regulator on Field Service Shoes with Fast Charge Method,” *MATRIK : Jurnal Manajemen, Teknik Informatika dan Rekayasa Komputer*, vol. 23, no. 2, pp. 273–284, Feb. 2024, <https://doi.org/10.30812/matrik.v23i2.3494>.
- [17] O. Alamu, A. Gbenga-Ilori, M. Adelabu, A. Imoize, and O. Ladipo, “Energy efficiency techniques in ultra-dense wireless heterogeneous networks: An overview and outlook,” *Engineering Science and Technology, an International Journal*, vol. 23, no. 6, pp. 1308–1326, Dec. 2020, <https://doi.org/10.1016/j.jestch.2020.05.001>.
- [18] A. F. Isnawati and M. Aly Afandi, “Game Theoretical Power Control in Heterogeneous Network,” in *2021 9th International Conference on Information and Communication Technology (ICoICT)*. Yogyakarta, Indonesia: IEEE, Aug. 2021, pp. 149–154, <https://doi.org/10.1109/ICoICT52021.2021.9527439>.

- [19] W. Lee, T.-W. Ban, and B. C. Jung, "Distributed Transmit Power Optimization for Device-to-Device Communications Underlying Cellular Networks," *IEEE Access*, vol. 7, pp. 87 617–87 633, 2019, <https://doi.org/10.1109/ACCESS.2019.2926310>.
- [20] F. H. Costa Neto, D. Costa Araujo, M. Pontes Mota, T. Maciel, and A. De Almeida, "Uplink Power Control Framework Based on Reinforcement Learning for 5G Networks," *IEEE Transactions on Vehicular Technology*, vol. 70, no. 6, pp. 5734–5748, Jun. 2021, <https://doi.org/10.1109/TVT.2021.3074892>.
- [21] A. F. Isnawati, "Feasibility Analysis of Distributed Power Control System for Cognitive Radio Networks," *Jurnal Nasional Teknik Elektro*, vol. 11, no. 1, pp. 29–35, Mar. 2022, <https://doi.org/10.25077/jnte.v11n1.994.2022>.
- [22] A. F. Isnawati, W. Pamungkas, and J. Hendry, "Power Control Game Performance in Cognitive Femtocell Network," *Journal of Communications*, pp. 121–127, 2019, <https://doi.org/10.12720/jcm.14.2.121-127>.
- [23] X. Li, J. Fang, W. Cheng, H. Duan, Z. Chen, and H. Li, "Intelligent Power Control for Spectrum Sharing in Cognitive Radios: A Deep Reinforcement Learning Approach," *IEEE Access*, vol. 6, pp. 25 463–25 473, 2018, <https://doi.org/10.1109/ACCESS.2018.2831240>.